Invited Paper

Towards a 0.24-THz, 1-to-2-MW-class gyrotron for DEMO

M. Thumm [1, 2*], J. Franck [1], P.C. Kalaria [1], K.A. Avramidis [1], G. Gantenbein [1], S. Illy [1], I.G. Pagonakis [1], M. Schmid [1], C. Wu [1], J. Zhang [1], and J. Jelonnek [1, 2],
Karlsruhe Institute of Technology (KIT), Kaiserstr. 12, 76131 Karlsruhe, Germany
[1] Institute for Pulsed Power and Microwave Technology (IHM)
[2] Institute of High Frequency Techniques and Electronics (IHE)
[*] Email: manfred.thumm@kit.edu

(Received August 18, 2015)

Abstract: Current design studies on electron cyclotron heating and current drive (ECH&CD) systems for a DEMO fusion reactor demand gyrotron frequencies of above 200 *GHz* for efficient CD and a total gyrotron efficiency above 60 % to achieve an efficient fusion power plant operation. Considering the mandatory total heating power for DEMO and the space and maintenance requirements per tube, gyrotrons with a unit power of above 1 *MW* will be needed. Furthermore, for plasma stability control using a simple fixed ECCD launcher, fast frequency tunability (in a few seconds) in steps of about 2-3 *GHz* is necessary. Such tubes require broadband or tunable output windows and their quasi-optical mode converter must support the conversion of the various modes to a fundamental Gaussian wave beam. Slow tunability of gyrotrons (within a few minutes) in leaps of about 30–40 *GHz* is considered advantageous (multi-frequency gyrotrons), e.g. for DEMO plasma start-up, for DEMO variants with a relatively low magnetic field or for multi-purpose use in other fusion devices such as ITER. A multi-frequency gyrotron can operate with a simple, single-disk synthetic-diamond output window which is transparent at the relevant frequencies.

Physical design studies towards DEMO-compatible 2 *MW*-class coaxial-cavity gyrotrons are being performed at KIT. A well suited coaxial-cavity mode series with good multi-frequency properties is:

$$TE_{35,21}\,(170\ GHz) – TE_{42,25}\,(203.8\ GHz) – TE_{49,29}\,(237.5\ GHz) – TE_{56,33}\,(271.3\ GHz).$$

At 237.5 *GHz* a coaxial-cavity design for the $TE_{49,29}$ mode has been found and optimized with quite promising results (1.9 *MW*, 33% electronic efficiency, without depressed collector (DC)). This frequency has been chosen such that the respective mode $TE_{35,21}$ exactly matches the ITER frequency of 170 *GHz*, allowing the gyrotron to be used for a later upgrade of the ITER ECH&CD system. The azimuthal neighboring modes of $TE_{49,29}$ have a frequency separation of 2 *GHz* and are well-suited fast frequency tuning. The design of the magnetron injection gun (MIG) has been finished, based on a realistic 10 *T* gyrotron magnet system.

As a backup solution, conceptual design studies on a hollow-cavity 1 *MW*-class gyrotron have also been performed. The current design permits multi-frequency operation with the following modes:

$$TE_{31,11}\,(170\ GHz) – TE_{37,13}\,(203\ GHz) – TE_{43,15}\,(236.1\ GHz) – TE_{49,17}\,(269.1\ GHz).$$

Numerical simulations with realistic electron beam velocity spread and beam width show, that about 1 *MW* output power at 36 % electronic efficiency (without DC) can be achieved.

The development of electron guns with high beam quality and of multi-stage depressed collectors (MSDC) for energy recovery is necessary to achieve the required overall gyrotron efficiency of above 60 %. KIT is installing a new gyrotron high-voltage power supply which will allow the operation of high-power gyrotrons with MSDCs.

Keywords: DEMO, Electron cyclotron heating and current drive (ECH&CD), Multi-frequency gyrotrons, Step-tunable gyrotrons, Mode selection, High-order modes, Magnetron injection gun, Quasi-optical mode converter, Broadband synthetic diamond Brewster and tunable windows.

doi: 10.11906/TST.085-100.2015.09.09

1. Introduction

From the technological point of view, electron cyclotron heating (ECH) is considered to be the most mature auxiliary heating method for ITER, due to the availability of reliable 1 *MW* continuous wave (CW) 170 *GHz* gyrotrons and to the simplicity of wave launching and wave-plasma coupling. However, electron cyclotron current drive (ECCD) alone is not sufficient for long-pulse discharges within the present ITER design because of the lower ECCD efficiency compared to ion cyclotron CD, lower hybrid CD and neutral beam CD. This is evident since the 170 *GHz* ECH system of ITER has not been designed with the main goal of maximizing the amount of ECCD efficiency [1]. Conversely, the ECH&CD system of a future, commercially attractive tokamak demonstration fusion reactor DEMO operating under pulsed (several hours) or stationary conditions must be optimized to provide maximum possible CD efficiency. The achievable ECCD efficiency in two DEMO scenarios has been investigated in [2], one for pulsed and one for steady state operation. Millimeter (mm)-wave beam propagation, absorption and current drive have been simulated employing beam-tracing techniques and including momentum conservation in electron-electron collisions. For mid-plane wave launching the achievable CD efficiency has been found to be limited by 2nd harmonic absorption. Higher efficiencies can be obtained by injecting the mm-wave beams from the top of the tokamak, using wave absorption by more energetic, less collisional electrons. CD efficiencies competitive with those usually achieved by neutral beam CD have been calculated. Assuming the EUROfusion 2012 baseline for DEMO (aspect ratio of 4.0 and B > 7 T) the operation frequencies for optimum ECCD are significantly above 200 *GHz*, while lower frequencies around 170 *GHz* and 200 *GHz* appear useful for plasma start-up and bulk heating.

Considering the mandatory total heating power for DEMO and the spacial and maintenance requirements per gyrotron, a gyrotron unit power of 1.5 to 2 *MW* would be advantageous. According to our present understanding, this can only be provided by very high-order volume mode coaxial-cavity gyrotrons [3], since Ohmic cavity wall loading scales with $f^{5/2}/[\chi^2(1-C_c^2)]$, where χ is the mode eigenvalue and $C_c = R_c/R_{cav}$ is the relative caustic radius of the mode (R_{cav} and R_c are the cavity and caustic radius, respectively). Furthermore, the longitudinally corrugated inner conductor in coaxial cavities reduces mode competition [3]. For neo-classical tearing mode (NTM) stabilization using simple fixed ECCD launchers, fast frequency tunability of the gyrotrons (within a few seconds) in steps of about 2-3 *GHz* is necessary [4], in conjunction with broadband Brewster or tunable chemical-vapor-deposition (CVD) diamond windows [5-11]. Slow frequency tunability (within a few minutes) in leaps of 30-40 *GHz* (termed multi-frequency operation), related to the transmission maxima of a plane single-disk CVD-diamond window, is considered advantageous for multi-purpose use of fusion gyrotrons, e.g. for a steady-state or a pulsed DEMO reactor or for upgrades of the ITER- and Wendelstein 7-X (W7-X) ECH systems.

Physical design studies towards DEMO compatible gyrotrons, including cavity, magnetron injection gun (MIG), quasi-optical output coupler and multi-stage depressed collector, are being performed at the Karlsruhe Institute of Technology (KIT). A coaxial gyrotron cavity design for the $TE_{49,29}$ mode at 237.5 *GHz* has been developed and optimized. The corresponding mode series with good multi-frequency properties is as follows:

$$TE_{35,21}\,(170\ GHz) – TE_{42,25}\,(203.8\ GHz) – TE_{49,29}\,(237.5\ GHz) – TE_{56,33}\,(271.3\ GHz).$$

The frequency has been chosen such that the allied mode $TE_{35,21}$ matches the ITER frequency of 170 *GHz* and the highest frequency mode $TE_{56,33}$ at around 271 *GHz* could be used for ECCD in a high-magnetic field DEMO version. The azimuthal neighboring modes of $TE_{49,29}$ have a frequency separation of 2 *GHz* and nearly the same radial location of the field maximum which is required for fast frequency tuning for NTM stabilization. The present paper describes the simulation results for the three lower modes of this series and the design of cavity and magnetron injection gun (MIG). The maximum achievable output power at very high frequencies will be determined by the continuously evolving boundaries of the core technologies, such as the maximum thermionic emission for long cathode lifetimes, thermal cavity and collector wall loading, efficiency of depressed collector (DC) and superconducting magnet technology.

As an alternative, more conservative solution, design considerations for a conventional 1 *MW* gyrotron are also in progress, based on a corresponding series of hollow-cavity modes:

$$TE_{31,11}\,(170.0\ GHz) – TE_{37,13}\,(203\ GHz) – TE_{43,15}\,(236.1\ GHz) – TE_{49,17}\,(269.1\ GHz).$$

In this case the first two modes at 170 *GHz* and 203 *GHz* and the allied modes $TE_{25,9}$ at 137 *GHz* and $TE_{19,7}$ at 104 *GHz* have already been successfully experimentally tested by the JAEA gyrotron team in Japan [12].

In both cases of coaxial or hollow-cavity gyrotron proper operation of the quasi-optical launcher (with radius R_L) and optimum coupling to the hollow electron beam can only be achieved when the relative caustic radii C_c and thus the absolute caustic radii R_c of the cavity modes are almost the same. Then also the Brillouin angles $\theta_B = \arccos[1 - (R_{cav}/R_L)^2]^{1/2}$, the azimuthal radiation spread angles $2\phi = 2\arccos(C_c)$ at the launcher cut and the required cut lengths $L = 2\pi R_L \sin\phi/(\phi \tan\theta_B)$ of the various modes are almost the same.

2. Design of a 2 MW coaxial-cavity gyrotron

KIT is working on the design for a 2 *MW* coaxial-cavity gyrotron, which can operate with good performance at 237.5 *GHz*. The cavity mode $TE_{49,29}$ is the result of an adequate mode-selection strategy considering quasi-optical output coupler and output window [13], allowing the modes $TE_{35,21}$ (170 *GHz*) and $TE_{42,25}$ (203.8 *GHz*) as secondary operating modes; see Fig. 1 for illustration. The priority of initial studies was the optimization of the cavity [14] and of the triode-type magnetron injection gun (MIG) [15] with respect to the $TE_{49,29}$ main design mode, using rather simplified assumptions for the electron beam.

In the following, we present the imposed technical design restrictions, realistic assumptions for the electron emission and corresponding simulation results for all three operating modes. For interaction and MIG simulations, the European proprietary codes SELFT [16] and EURIDICE [17], and ARIADNE [18] and ESRAY [19], respectively, were used.

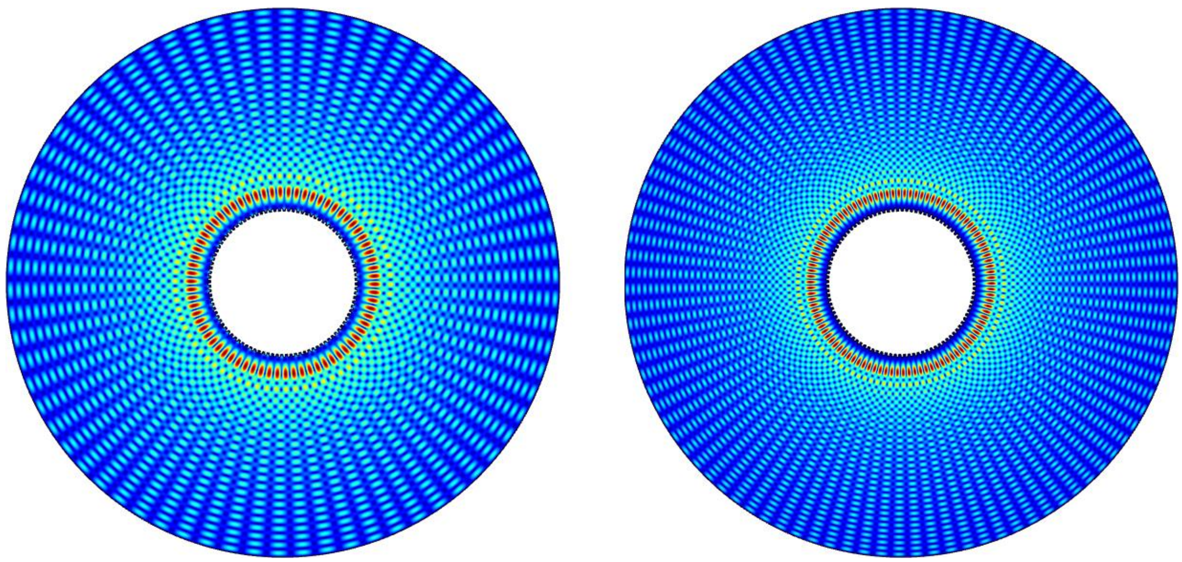

Fig. 1 Transversal intensity profiles of the non-rotating modes $TE_{35,21}$ and $TE_{49,29}$.

Table 1 summarizes the features of the chosen cavity mode series with 1.854 *mm* thickness of the CVD-diamond window disk (- 20 *dB* reflection bandwidth = 2.2 *GHz*). The maximum deviation of C_c is 0.26%, which leads to a maximum horizontal shift of the mm-wave output beam from the window center of the order of only 50 *μm* [20] and thus allows to use the same beam matching optics for all the different operating modes. Table 2 shows the cavity mode spectrum for frequency tunable operation in 2 GHz steps over a bandwidth of 18 *GHz* around the center mode. Here the maximum deviation of C_c is 2.5% resulting in a maximum horizontal beam shift of the order of 2 *mm* [20, 21].

Tab. 1 Properties of operating modes of a multi-purpose, multi-frequency coaxial-cavity gyrotron with 1.854 *mm* thick single-disk CVD-diamond vacuum window together with possible fusion plasma applications (UG: Upgrade) [21].

Frequency [*GHz*] Application	170.0 ITER UG	203.8 ITER UG CD	237.5 DEMO	271.3 DEMO CD
Cavity Mode Bessel Zero Relative Caustic Radius C_c	$TE_{35,21}$ 113.1329 0.3094	$TE_{42,25}$ 135.5957 0.3097	$TE_{49,29}$ 158.0584 0.3100	$TE_{56,33}$ 180.5209 0.3102
Normalized Window Thickness [λ]	5/2	6/2	7/2	8/2
Window Center Frequency [*GHz*]	169.6	203.6	237.5	271.4

Tab. 2 Properties of operating modes of a frequency step-tunable coaxial-cavity gyrotron with broadband or tunable CVD-diamond vacuum window [21].
Frequency band: 228.6 *GHz* < *f* < 246.4 *GHz*. Frequency steps: Δf = 2 *GHz*.

Freq. [*GHz*] Δf [*GHz*]	228.6 2.0	230.6 2.0	232.5 1.0	233.5 2.0	235.5 2.0	237.5	239.5 2.0	241.5 2.0	242.5 1.0	244.5 2.0	246.4 2.0
Cavity Mode	$TE_{47,28}$	$TE_{48,28}$	$TE_{49,28}$	$TE_{47,29}$	$TE_{48,29}$	$TE_{49,29}$	$TE_{50,29}$	$TE_{51,29}$	$TE_{49,30}$	$TE_{50,30}$	$TE_{51,30}$
C_c	0.309	0.313	0.317	0.302	0.306	0.310	0.314	0.317	0.304	0.307	0.311

2.1. Design assumptions

In the preceding study, the maximum current density of the temperature limited Tungsten dispenser cathode emitter of the MIG was set to 4 *A/cm*^{2}. With an emitter radius of 65 *mm*, a slant angle of 25° and an emitter width of 4.3 *mm* (3.9 *mm* width projected to the gyrotron axis), 70 *A* of electron beam current can be achieved. The pitch factor α (ratio of perpendicular and parallel velocity component) of the electrons has been assumed to be around 1.25. The beam energy for $TE_{49,29}$-mode operation is limited by the permitted maximum Ohmic loading on the cavity walls (2.0 *kW/cm*^{2} at the outer wall and 0.2 *kW/cm*^{2} on the coaxial insert) and was taken as the upper boundary for all three operating modes. For $TE_{49,29}$-mode operation and with an appropriate MIG design (see Fig. 2), one obtains an rms spread in the perpendicular velocity component ($\delta_{\beta,perp}$) of the electrons of around 1 % at the cavity entrance, which has no significant influence on the interaction efficiency [22]. However, additional spread has to be considered from the emitter surface roughness [23] and from possible further non-uniform emission (caused by non-uniform heating or a non-uniform work-function distribution). In $TE_{49,29}$-mode operation, a typical emitter structure size of 2 *μm* leads to an increase of $\delta_{\beta,\mathrm{perp}}$ to 3.4 %. For interaction calculations, $\delta_{\beta,\mathrm{perp}}$ = 6 % was assumed, which means that less than 3 % spread may result from azimuthal variations of cathode work function and heating temperature. These beam parameters allow generation of 1.9 *MW* mm-wave power at 33 % electronic efficiency.

The MIG has been designed such that reflection and trapping of secondary electrons is avoided for all three operating modes. Despite its relative compactness, the electric field within the MIG nowhere exceeds 7 *kV/mm* on its metallic surfaces.

An initial design for a 10.5 *T* magnet with 270 *mm* warm bore-hole diameter, supplied by an industrial manufacturer, has been used for the simulations.

The considered cavity has a radius of 31.78 *mm* and a length of 15 *mm* (straight middle section, including initial parts of the parabolic smoothenings). The conical coaxial insert in this region has 100 longitudinal corrugations (each having a depth of 0.3 *mm*) and a radius between 8.66 *mm* (cavity entrance) and 8.4 *mm* (cavity exit).

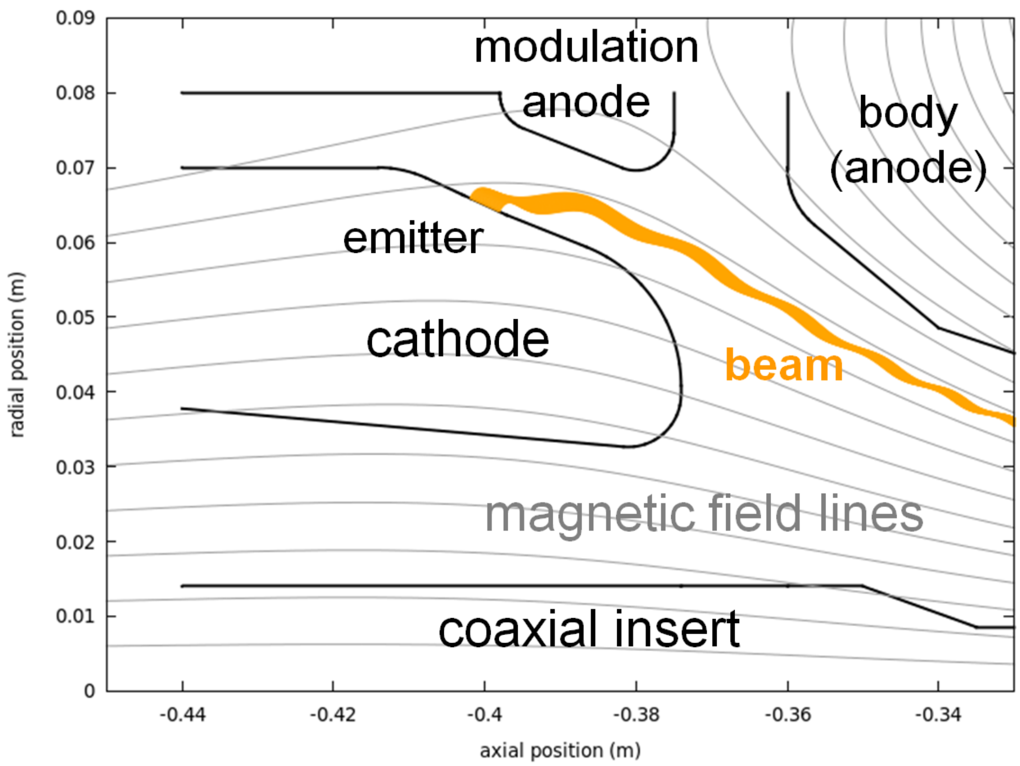

Fig. 2 Triode-type MIG design of the coaxial cavity-gyrotron, including magnetic field lines and the electron beam for operation in the $TE_{49,29}$ mode at 237.5 *GHz* [22].

2.2. Design results

Table 3 shows the operating points and simulation results for the three frequencies under consideration. These values have been found using self-consistent time-dependent start-up simulations with at least ten modes each, taking into account the full guiding center distribution, velocity spread and voltage depression of the electron beam; see Fig. 3 for the $TE_{49,29}$-mode start-up. While the optimum electron beam radius in the cavity is almost constant and likewise is the overall magnetic field profile, the modulation anode voltage has to be varied significantly to compensate the different magnetic field strengths at the emitter in order to obtain a reasonable pitch factor.

Due to its own space-charge, the electron beam experiences a voltage depression between emitter and cavity, but it is well known that, compared to a hollow-cavity set-up, this depression is significantly reduced by the coaxial insert. As one can see from Table 3, the voltage depression is only around 2 *kV* for all three operating modes.

The peak Ohmic loading of the longitudinally corrugated coaxial insert for the various operating modes should be considered carefully, see Table 4: While the loading on the outer cavity wall decreases with decreasing operating wavelength at otherwise similar operating parameters, the loading on the insert increases. This is due to the broader mode maximum for lower-order modes.

Tab. 3 Operating parameters of the three operating coaxial-cavity modes [22].

Window thickness in multiples of $\lambda/2$	5	6	7
Operating mode	$TE_{35,21}$	$TE_{42,25}$	$TE_{49,29}$
Mode eigenvalue	113.1	135.6	158.1
Frequency [*GHz*]	170.0	203.8	237.5
Magnetic field at emitter [*T*]	0.137	0.165	0.191
Accelerating voltage [*kV*]	85.6	87.9	87.4
Modulation anode voltage [*kV*]	53.7	46.6	37.5
Beam current [*A*]	69.4	70.0	69.3
Velocity spread by MIG [%]	6.8	4.3	3.4
Magnetic field in cavity [*T*]	6.82	8.22	9.58
Beam voltage [*kV*]	83.4	86.0	85.6
Velocity spread (interaction sim.) [%]	8	6	6
Guiding center radius at cavity [*mm*]	10.28	10.27	10.24
Pitch factor at cavity	1.27	1.25	1.22
Wavelength-to-beam-thickness ratio (in cavity)	6.2	5.1	4.4
Output power [*MW*]	1.8	1.9	1.9
Electronic efficiency [%]	31	32	33

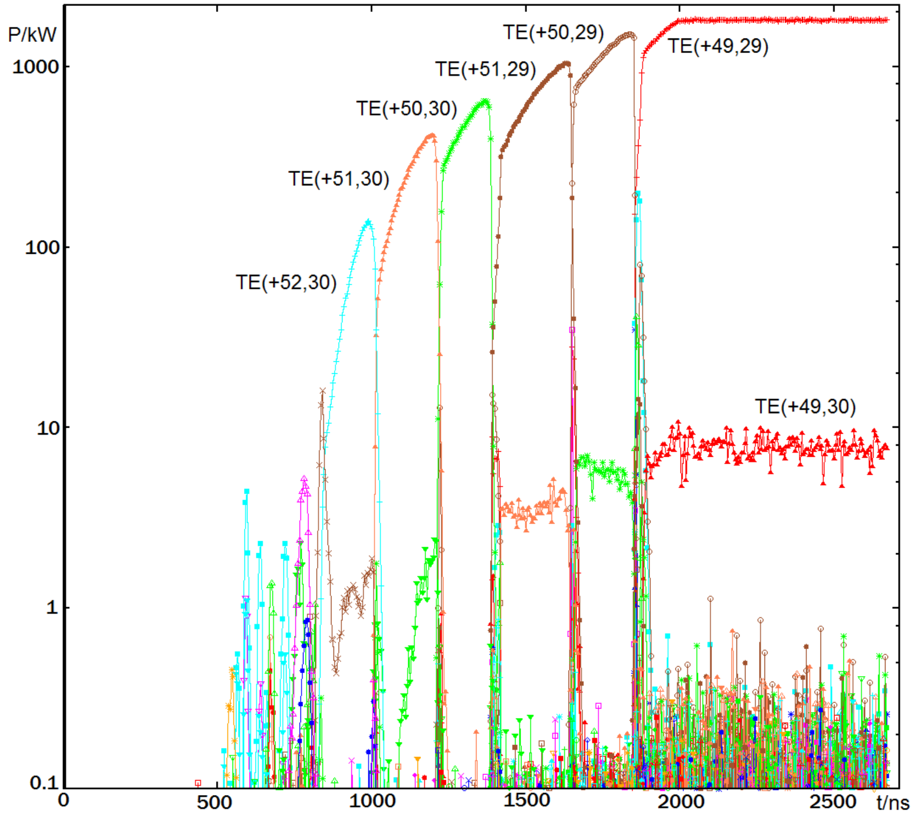

Fig. 3 Startup scenario for operation in the $TE_{49,29}$ mode at 237.5 *GHz*. The voltages have been ramped up linearly, with the beam current following according to the Schottky effect. At t = 2000 *ns* simulation time, the ramp-up was discontinued as the design values were reached [22]. Modes co-rotating with the electrons are marked by a plus sign, counter-rotating modes by a minus sign.

Tab. 4 Peak loading for the three operating coaxial-cavity modes [22].

Operating cavity mode	$TE_{35,21}$	$TE_{42,25}$	$TE_{49,29}$
Cavity wall loading [kW/cm^2]	1.3	1.7	2.0
Coaxial insert loading [kW/cm^2]	0.5	0.3	0.2

3. Design of a 1 MW hollow-cavity gyrotron

3.1. Multi-frequency operation

In order to provide an alternative, more conservative design, studies on a corresponding hollow-cavity gyrotron have been performed at KIT employing the mode selection approach for high-frequency, high-power DEMO gyrotrons described in [14] where considerations of multi-frequency operation of the tube are included [21]. After successful selection of the operating mode, the physical design is going to be finalized [24, 25]. The simulated performance results of the hollow-cavity gyrotron for multi-frequency operation are listed in Table 5. Possible operating frequencies with their applications and the operating modes are also mentioned. An electron pitch factor of 1.25 and a cavity wall loading of 2 kW/cm^2 have been assumed in the basic design. Output power and efficiency were calculated considering an ideal electron beam. For comparison, results for a typical realistic electron beam with velocity spread and radial width are also shown and are further discussed in the next section. The code package EURIDICE [17] has been used for the simulations.

Tab. 5 Multi-frequency operation of the proposed hollow-cavity gyrotron with the simulated performance parameters and possible applications (H: plasma heating, CD: current drive, A: DEMO aspect ratio) [25].

Frequency [GHz]	170.0	203.0	236.1	269.1
Applications	H, A=3.1	H, A=3.6 CD, A=3.1	H, A=4.0 CD, A=3.6	CD, A=4.0
Mode	$TE_{31,11}$	$TE_{37,13}$	$TE_{43,15}$	$TE_{49,17}$
Mode Eigenvalue	74.325	88.769	103.213	117.656
Magnetic field [T]	6.731	7.892	9.130	10.317
Beam Radius [mm]	9.13	9.10	9.06	9.04
Beam Voltage [keV]	74	62	58	52
Beam Current [A]	52	44	39	35
Wall Loading [kW/cm^2]	2.01	2.01	1.99	1.99
Without consideration of velocity spread and radial electron beam width				
Output Power [kW]	1260	980	828	690
Interaction Efficiency [%]	33	36	38	40
With 6% velocity spread and 2*Larmor radius radial electron beam width				
Output Power [kW]	1170	918	775	648
Interaction Efficiency [%]	31.5	35.0	36.0	37.0

3.2. Realistic electron beam parameters

At the initial stage of the hollow-cavity design, an ideal, infinitesimally thin electron beam without velocity spread was considered. In reality, the electron beam generated by a MIG has a certain velocity spread and a finite radial width. That makes it necessary to verify the gyrotron performance with realistic electron beam parameters. Output power and efficiency of the gyrotron with several normalized velocity spreads are shown in Table 6. The electron velocities were distributed over the total number of electrons via a Gaussian function. Output power and efficiency decrease with increasing velocity spread, but the operating mode remains stable. The multi-mode start-up scenario with 6 % velocity spread is shown in Fig. 4. Here, a negative azimuthal index denotes that the mode is co-rotating with the electrons. Gyrotron operation with various radial beam widths is summarized in Table 7. The values of radial width represent a single-side guiding center spread. Here, the Larmor radius R_L = 71.4 μm and the wavelength λ = 1.271 mm. Fig. 5

shows the mode evolution in the case of different radial widths. The output power is not affected significantly by an increase in the radial width, but after a certain threshold value, the operating mode is no longer stable at the design parameters.

Tab. 6 Operation of the proposed 236 *GHz*,$TE_{43,15}$-mode gyrotron considering a non-ideal electron beam [25].

$\beta_\perp$ spread (*rms*) [%]	α spread (*rms*) [%]	Output power P_{out} [*kW*)]	Efficiency η [%]
0	0	828	38.0
6	15.4	778	36.1
8	20.5	744	34.7
10	25.6	700	33.4

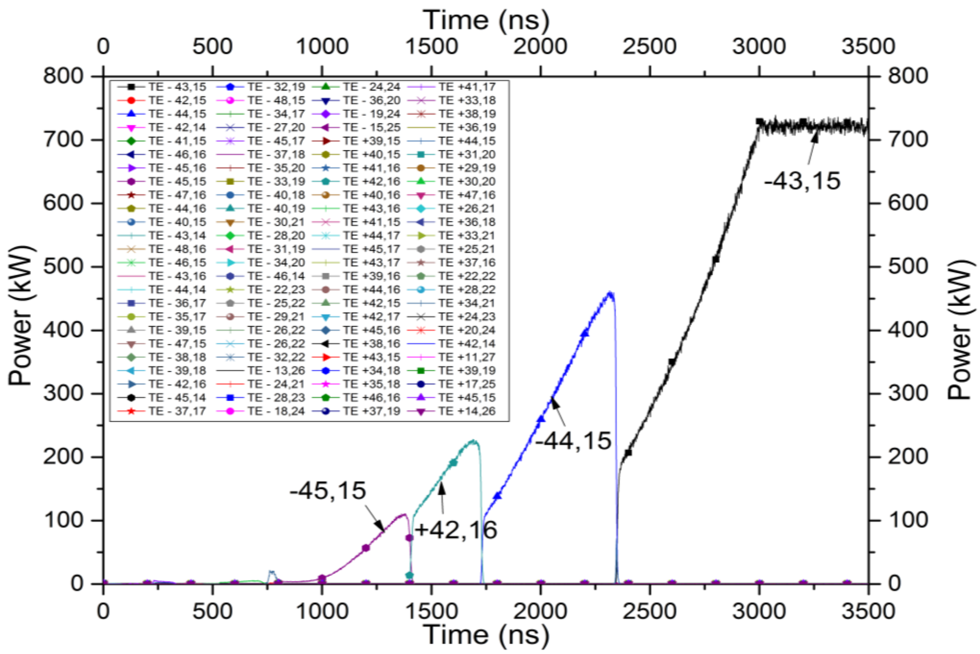

Fig. 4 Start-up scenario for the conventional hollow-cavity gyrotron assuming 6 % velocity spread [25].

Tab. 7 Effect of radial electron beam width on the operation of a conventional hollow-cavity 236 *GHz* 1-*MW*-class DEMO gyrotron [25].

Radial Width [R_L]	Radial Width [λ]	Radial Width [%]	Output Power P_{out} [*kW*]	Efficiency η [%]
2	λ/8.8	1.6	827	37.7
3	λ/5.9	2.4	821	37.5
4	λ/4.4	3.2	815	37.2
5	λ/3.6	3.9	801	36.5
6	λ/3.0	4.7	Unstable mode	

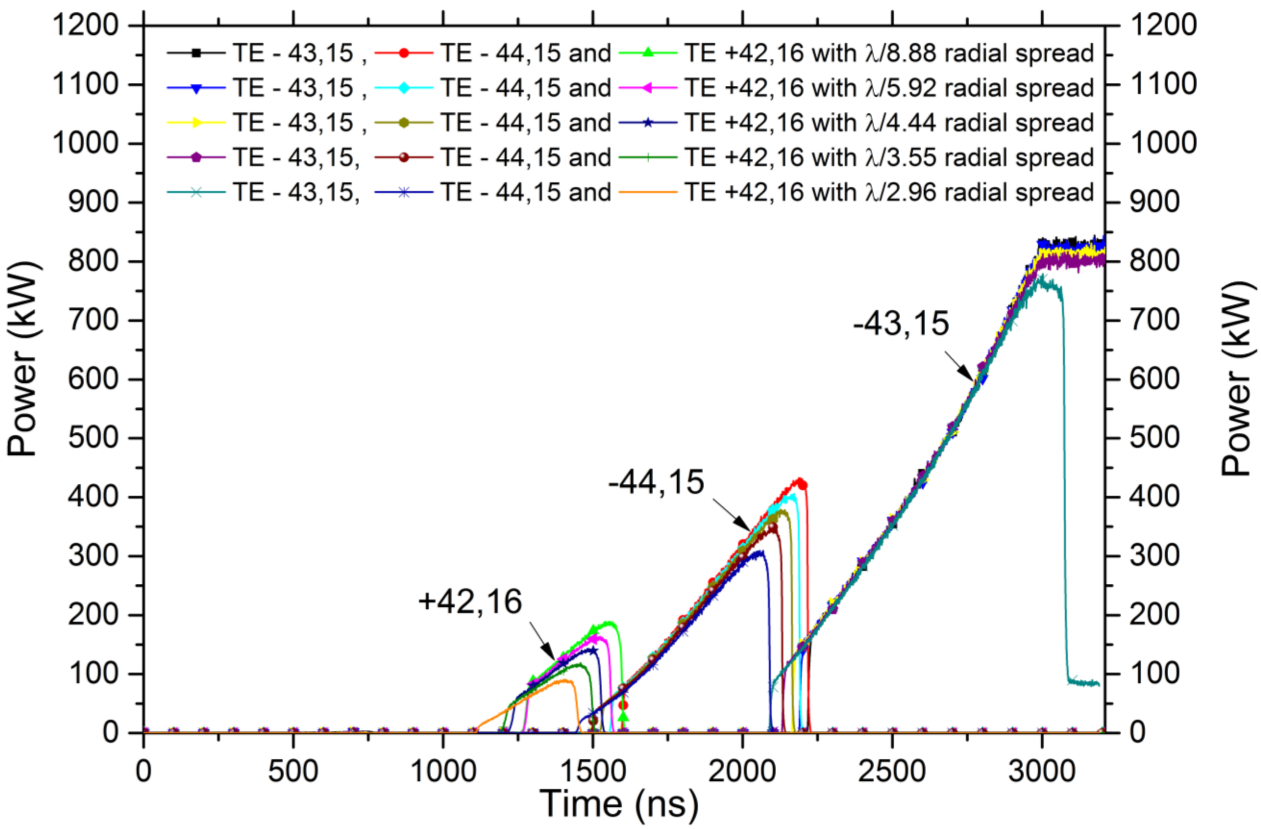

Fig. 5 Result of self-consistent, time-dependent multi-mode calculations with consideration of different radial electron beam width [25].

An increase of the permitted maximum Ohmic cavity wall loading by improved cooling technologies, of course would allow to achieve higher output power. Table 8 summarizes the values of output power, efficiency, accelerating voltage and electron beam current for three different levels of maximum cavity loading.

Tab. 8 Operational parameters of the proposed conventional hollow-cavity 236 *GHz* $TE_{43,15}$-mode gyrotron considering different values of maximum Ohmic cavity wall loading [24].

Wall loading [kW/cm^2]	Output power [*kW*]	Efficiency [%]	Beam voltage [*kV*]	Beam current [*A*]
2.00	828	38.0	58	39
2.30	990	39.2	60	42
2.48	1080	38.5	60	47

4. Multi-stage depressed collector

One possibility to improve the total efficiency of a gyrotron above 60 % is to use a multi-stage depressed collector (MSDC). That technology is well known from highly efficient traveling wave tubes (TWT) for space applications [26]. Those collectors use electrostatic or magnetic focusing to separate electrons with different energies of the spent electron beam in several intermediate steps of the depression voltage along the electron beam axis. According to the authors' best knowledge, in case of gyrotron operation there are only two known theoretical MSDC concepts of MSDC: one is making use of the non-adiabatic electron trajectories in a strong magnetic field; the other is using the ***E x B*** drift of the electrons [27]. Even though several considerations about MSDC designs for gyrotrons exist in the literature (e.g. [28]), there is not any successful implementation of that technology in an experimental gyrotron.

In the frame of EUROfusion at KIT, the MSDC technology shall be pushed significantly forward. Initial steps towards new design concepts towards feasible MSDC versions have already been undertaken. For example, the theoretical optimal efficiency depending on the distribution of the electron energy has been calculated and some conceptual simulations have been made.

KIT is currently adding a new gyrotron test facility, called Fusion Long Pulse Gyrotron Laboratory (FULGOR) [29], to the existing one. Initially FULGOR will comprise of a 10 *MW* CW power supply (consisting of 70 to 80 enhanced pulse step modulator modules, providing up to - 90 *kV* accelerating voltage, 120 *A* beam current, 3600 *s* pulse duration, 50 % duty cycle, rise time < 50 *μs*, up to 5 *kHz* modulation and arc energy deposition < 10 *J*), and stable intermediate voltage taps. Furthermore a 5 *MW* water cooling system (upgradeable to 10 *MW*), a superconducting 10 *T* magnet, one or two 2 *MW* ECRH test loads and a new control and data acquisition system for all these elements form part of the new facility. The design of the new high voltage DC power supply (HVDCPS) is flexible enough to handle gyrotrons with 4 *MW* CW output power (conceivably up to 170 *GHz* [30]), but also to test gyrotrons with higher frequencies (> 200 *GHz*) which, due to physical limitations in the gyrotron design, will require less power but have more stringent demands on voltage stability. The HVDCPS will also be capable of supplying MSDC gyrotrons (see Fig. 6). Thus, the test facility will be equipped to test the hollow-cavity 1 *MW* or coaxial-cavity 2 *MW* gyrotrons for DEMO as well as possible upgraded gyrotrons for W7-X and ITER. FULGOR should become operational within the next three years.

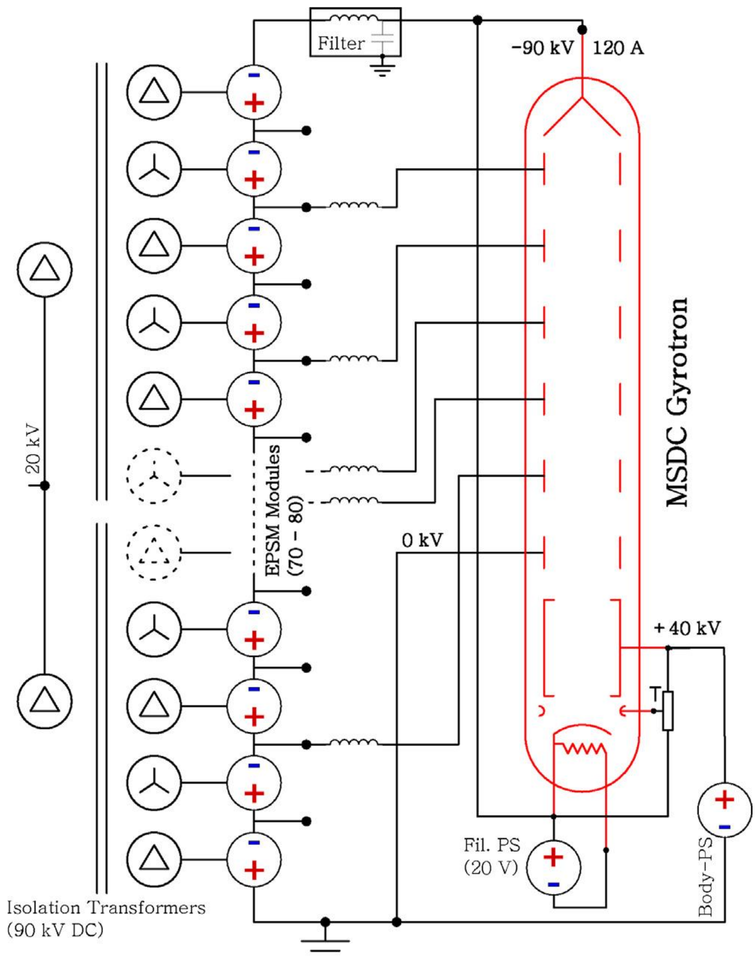

Fig. 6 High voltage DC power supply configuration with intermediate tabs for multi-stage depressed collector (MSDC) gyrotons [29].

5. Conclusions

DEMO-compatible multi-frequency high-power gyrotrons with the main operating frequency at around 240 *GHz* are under development at KIT in the framework of the EUROfusion Consortium. Time-dependent, self-consistent multi-mode interaction simulations have been performed, including a realistic electron beam velocity spread and beam width. In the basic designs, the permitted maximum Ohmic loading of the cavity wall was limited to 2 kW/cm^2.

Coaxial-cavity tubes can generate 1.9 *MW* mm-wave power in CW operation at 33 % electronic efficiency (without depressed collector). Their multi-frequency behavior has been investigated. While the triode-type magnetron injection gun design for the three chosen operating modes $TE_{49,29}$ at 237.5 *GHz*, $TE_{42,25}$ at 203.8 *GHz* and $TE_{35,21}$ at 170.0 *GHz* is promising and the interaction at the main mode $TE_{49,29}$ is robust, the Ohmic loading of the coaxial insert increases for operation at the lower frequencies. An optimized coaxial-cavity, multi-frequency gyrotron would thus require a thinner insert (which, however, might somewhat increase mode competition for the $TE_{49,29}$ main mode at 237.5 *GHz*) and/or should be operated at lower power for the lower frequencies.

As an alternative approach, conceptual design studies on a corresponding conventional 1-*MW*-class gyrotron with cylindrical hollow cavity have also been undertaken. Here, the main mode is $TE_{43,15}$ at 236.1 *GHz* and the lower frequency modes are $TE_{37,13}$ at 203.0 *GHz* and $TE_{31,11}$ at 170.0 *GHz*. Operation at 269.1 *GHz* in the $TE_{49,17}$ mode also has been studied. 1 *MW* CW power at 236.1 *GHz* can be achieved with an electronic efficiency of 36 % (without depressed collector).

The development of magnetron injection electron guns with high beam quality and of multi-stage depressed collectors for efficient energy recovery is under progress at KIT in order to achieve the required total gyrotron efficiency of above 60 %.

Acknowledgments

This work has been carried out within the framework of the EUROfusion Consortium and has received funding from the Euratom research and training programme 2014-2018 under grant agreement No 633053. The views and opinions expressed herein do not necessarily reflect those of the European Commission.

Parts of the simulations presented in this work have been carried out using the HELIOS supercomputer at IFERC-CSC.

References

[1] T. Imai, N. Kobayashi, R. Temkin, et al.. "ITER R&D: auxiliary systems: electron cyclotron heating and current drive system". *Fusion Eng. and Design*, 55, 281-289 (2001).

[2] E. Poli, G. Tardini, H. Zohm, et al.. "Electron-cyclotron-current-drive efficiency in DEMO plasmas". *Nucl. Fusion*, 53, 013011 (10 pp) (2013).

[3] B. Piosczyk, O. Braz, G. Dammertz, et al.. "A 1.5-MW, 140 GHz, TE28,16-coaxial cavity gyrotron". *IEEE Trans. on Plasma Science*, 25, 460-469 (1997).

[4] H. Zohm and M. Thumm. "On the use of step-tuneable gyrotrons in ITER". *J. of Phys.: Conf. Series*, 25, 274-282 (2005).

[5] O. Braz, G. Dammertz, M. Kuntze and M. Thumm. "D-band frequency step-tuning of a 1 MW gyrotron using a Brewster output window". *Int. J. of Infrared and Millimeter Waves*, 18, 1465-1477 (1997).

[6] M. Thumm. "Development of output windows for high-power long-pulse gyrotrons and EC wave applications". *Int. J. of Infrared and Millimeter Waves*, 19, 3-14 (1998).

[7] B. Piosczyk, A. Arnold, G. Dammertz, et al.. “Step-frequency operation of a coaxial cavity gyrotron from 134 to 169.5 GHz”. *IEEE Trans. on Plasma Science*, 28, 918-923 (2000).

[8] M. Thumm, A. Arnold, E. Borie et al.. “Frequency step-tunable (114-170 GHz) megawatt gyrotrons for plasma physics applications”. *Fusion Eng. and Design*, 53, 407-421 (2001).

[9] V.E. Zapevalov, A.A. Bogdashov, G.G. Denisov, et al.. “Development of a prototype of a 1-MW 105-156-GHz multifrequency gyrotron”. *Radiophysics and Quantum Electronics*, 47, 396-404 (2004).

[10] I.V. Kazansky, A.V. Kruglov, S.A. Malygin, et al.. “Step-tunable experimental gyrotrons at 75 GHz and 140 GHz ranges”. *Proc. 7th Int. Workshop on Strong Microwaves: Sources and Applications*, Nizhny Novgorod, 2008, 1, 100-102 (2009).

[11] A.G. Litvak, G.G. Denisov, V.E. Myasnikov, et al.. “Recent development resulrs in Russia of megawatt power gyrotrons for plasma installations”. *EPJ Web of Conferences*, 32, 04003 (5pp) (2012).

[12] Y. Oda, K. Kajiwara, K. Takahashi, et al.. “Development of dual frequency gyrotron and high power test of EC componants”. *EPJ Web of Conferences*, 32, 04004 (8pp) (2012).

[13] J. Franck, K. A. Avramidis, G. Gantenbein, et al.. “A generic mode selection strategy for high-order mode gyrotrons operating at multiple frequencies”. *Nucl. Fusion*, 55, 013005 (2015).

[14] J. Franck, S. Illy, K Avramidis, et al.. “Mode selection and resonator design for DEMO gyrotrons”. *Proc. 15th IEEE Int. Conf. on Vacuum Electronics (IVEC 2014)*, Monterey, CA, USA, 31-32 (2014).

[15] J. Franck, I. Gr. Pagonakis, K. A. Avramidis, et al.. “Magnetron injection gun for a 238 GHz 2 MW coaxial-cavity gyrotron”. *9th German Microwave Conference*, Nuremberg, Germany, Talk S15.2 (2015).

[16] S. Kern. “Numerical Codes for interaction calculations in gyrotron cavities at FZK”. *Proc. 21st Int. Conf. Infrared and Millimeter Waves (IRMMW 1996)*, Berlin, Germany, Invited Paper AF2 (1996).

[17] K. A. Avramidis, I. Gr. Pagonakis, C. T. Iatrou, and J. L. Vomvoridis. “EURIDICE: A code-package for gyrotron interaction simulations and cavity design”. *EPJ Web of Conferences*, 32, 04016 (2012).

[18] I. Gr. Pagonakis and J. L. Vomvoridis. “The self-consistent 3D trajectory code ARIADNE for gyrotron beam tunnel simulation”. *Conf. Digest 29th IRMMW-THz*, Karlsruhe, Germany, 657-658 (2004).

[19] S. Illy, J. Zhang, and J. Jelonnek, “Gyrotron electron gun and collector simulation with the ESRAY beam optics code”, *Proc. 16th IEEE Int. Conf. on Vacuum Electronics (IVEC 2015)*, Beijing, China, Talk P1.1 (2015).

[20] O. Prinz, A. Arnold, G. Gantenbein, et al.. “Highly efficient quasi-optical mode converter for a multifrequency high-power gyrotron”. *IEEE Trans. on Electron Devices*, 56, 828-834 (2009).

[21] M. Thumm, J. Franck, S. Illy, et al.. “Towards a High-Power Millimeter-Wave Gyrotron for DEMO”. *Proc. 5th Int. Workshop on Far-Infrared Technologies (FIRT 2014)*, Fukui, Japan, 5-16, (2014)..

[22] J. Franck, K.A. Avramidis, I.Gr. Pagonakis, et al.. “Multi-frequency design of a 2 MW coaxial-cavity DEMO gyrotron”. *Proc. 40th Int. Conf. on Infrared, Millimeter, and Terahertz Waves (IRMMW-THz 2015)*, Hong Kong, Paper MS-16 (2015).

[23] J. Zhang, S. Illy, I.Gr. Pagonakis, et al. “Evaluation of gyrotron cathode emission inhomogeneity from current-voltage characteristics”. *16th IEEE International Vacuum Electronics Conference (IVEC 2015)*, Beijing, P.R. China, Paper S27.5 (2015).

[24] P.C. Kalaria, K. A. Avramidis, J. Franck, et al.. "Interaction circuit design and RF behavior of a 236 GHz gyrotron for DEMO". *9th German Microwave Conference*, Nuremberg, Germany, Talk S15.3 (2015).

[25] P.C. Kalaria, K.A. Avramidis, J. Franck, et al.. "Multi-frequency operation of DEMO gyrotron with realistic electron beam parameters". *16th IEEE International Vacuum Electronics Conference (IVEC 2015)*, Beijing, P.R. China, Paper S23.4 (2015).

[26] G. Faillon, G. Kornfeld, E. Bosch, and M. Thumm. "Microwave Tubes", in "Vacuum Electronics – Components and Devices". eds. J.A. Eichmeier and M. Thumm, Springer, Berlin Heidelberg New York, 1-84 (2008).

[27] I.Gr. Pagonakis, J.-P. Hogge, S. Alberti, et al.. "A new concept for the collection of an electron beam configured by an externally applied axial magnetic field". *IEEE Trans. on Plasma Science*, 36, 469-480 (2008).

[28] R.L. Ives, A. Singh, M. Mizuhara, et al.. "Design of a multistage depressed collector system for 1-MW CW gyrotrons-Part II: System consideration". *IEEE Trans. on Plasma Science,* 27, 503-511 (1999).

[29] M. Schmid, J. Franck, P. Kalaria, et al.. "Gyrotron development at KIT: FULGOR test facility and gyrotron concepts for DEMO". *Fus. Eng. and Design (2015)*, http://dx.doi.org/j.fusengdes.2015.03.003.

[30] M.H. Beringer, S. Kern and M. Thumm. "Mode selection and coaxial cavity design for a 4 *MW* 170 *GHz* gyrotron including thermal aspects". *IEEE Trans. on Plasma Science*, 41, 853-861 (2013).